

Interest of square voltages for Solid State Transformer operation with Grain Oriented Electrical Steel wound core

Sidi Hamdinou^{a,*}, Mathieu Rossi^a, Daniel Roger^a and Thierry Belgrand^b

^aUniv. Artois, EA4025, LSEE, 62400 Béthune, France

^bthyssenkrupp Electrical Steel, 62330 Isbergues, France

ARTICLE INFO

Keywords:

Grain Oriented Electrical Steel (GOES), Solid-State Transformers (SST), Eddy currents losses. Rectangular and square voltage comparison.

ABSTRACT

This paper presents a comparison between core losses within Grain Oriented Electrical Steel (GOES) wound core, under sinusoidal and rectangular voltage excitations at the same operating frequency and peak flux density.

Firstly, results issued by finite elements modeling and measurements are presented and discussed. Secondly, Fourier series are used to calculate the losses induced by the square voltage by adding the contribution of its harmonics, then compared to the sinusoidal case. The different approaches show that for the same operating frequency and induction, the losses under square excitation are lower than the sinusoidal one, this result is the main topic of this paper.

1. Introduction

Grain Oriented Electrical Steel (GOES) is a well-known magnetic material technology able to operate at high flux densities and low losses. GOES is available in thin sheets with an inorganic coating providing a high electrical insulation and keeps its properties even at very high operating temperatures. GOES has a particular crystalline texture produced by the mechanism of secondary recrystallization obtained during a specific high temperature long time annealing, leading to very large grains [1]. This texture provides optimal magnetic properties in the rolling direction [2]. Therefore, the thin sheets of GOES can be used for building high-performance wound cores able to operate at high flux densities and high temperatures.

Until now, GOES core has been mostly used in grid frequency power transformers [3], which are crucial elements of the conventional ac grid based on a centralized production system. The stability of the conventional grid is provided by the large power of a limited number of sources. The nodes of the grid are made by standard transformers associated with mechanical on-load tap changers [4].

Nowadays, the societal concerns about global warming impose an increasing part of renewable energy sources in the electric grid for reducing the share of fossil energy as coal, petroleum and gas. These renewable energy sources are known to be intermittent and decentralized; hence, the electrical grid is becoming more complex and the stability with fewer large and stable sources is at stakes [5, 6].

Such electric grids need smart nodes able to control the energy flow in real time. Solid-State Transformers (SST) are becoming key components of such smart nodes because they can be the power element of a large control system [7]. One of the main components of an SST is the transformer working at medium or high frequency for getting a high power transfer in a small volume. The transformer is the link be-

tween the static converters; it ensures the galvanic insulation and the voltage change.


In the most reported cases [8, 9, 10, 11] the transformer core of SSTs are built with amorphous or nanocrystalline materials operating at limited flux densities and associated with advanced SiC static converters. This combination allows high frequency operations and, consequently, very high power densities. However, the systems are complex and the design of large power SST cells is still difficult and expensive.

Widespread and mature material such as GOES can be used to design SST transformer cores and leading to an overall lower cost. With thin-gauge laminations [12], the wound core can operate at high peak flux densities and medium frequencies, in the kHz range. Therefore, associated with traditional Si-based converters, such Medium Frequency Transformers (MFT) can form high power SSTs with an excellent technical and economic balance. Fig. 1 illustrates a possible modular structure for designing a high power SST that can be used as a high power smart node connecting two dc grids. With such a structure the power flow between the two grids can be controlled on both directions in real time. Each SST cell is made of a MFT connected between two H-bridge converters working in rectangular voltage waves. The cells are connected in series for the high voltage (HV) side and in parallel for the low voltage (LV) one.

The paper presents a part of a study made on a MFT built with GOES wound core and fed by simple converters producing rectangular voltage waves in the kHz range. The aim of the study is to understand the behaviour of the transformer wound core and figure out its limits in terms of operating frequency and peak flux density. The experimental cores are made of 0.18 mm GOES sheets wound on a mandrel and annealed for suppressing the mechanical stresses.

The paper focuses on the core losses induced rectangular voltage compared to sine ones at the same peak flux density and frequency. It begins by an experimental approach on a wound GOES core operating in the kHz range for various

*Principal corresponding author

 shmaminou.hamdinou@univ-artois.fr (S. Hamdinou)

ORCID(s):

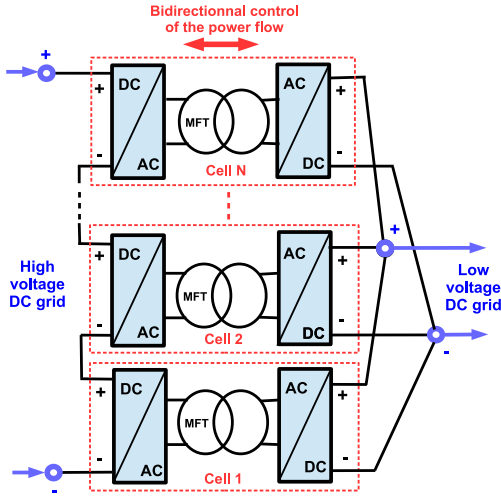


Figure 1: Modular structure of a large power SST.

peak flux densities. Then an interpretation base on Fourier series is proposed. Finally, the paper proposes an interpretation using a finite elements (FE) model that takes into account the non-linear behaviour of the GOES.

2. Core losses measurements

Measurements are performed on a MFT prototype shown in fig.2. The prototype windings are made with a high temperature wires insulated by an inorganic coating made of mica and fiberglass that can operate up to 500°C . With such a winding technology, the coil temperature enables to reach a wide range of induction level and frequencies under rectangular and sine voltages excitation.

Fig.3 show the test bench bloc diagram. The H-bridge dc-ac converter produces naturally a rectangular voltage rectangular wave, which magnitude depends on the dc bus. The H-bridge converter is controlled accurately by the mean of a micro-controller for getting a strictly null mean voltage. The high magnitude rectangular voltage wave can be used directly for measurements under rectangular voltage or filtered for operating in sine waves. For sine measurements a low-pass LC circuit is inserted between the H-bridge converter and the transformer under tests. The filter is used on the -40dB/decade slope; the voltage reduction is compensated by a corresponding increase of the dc input source.

For both cases, the current wave forms are measured with a non inductive high accuracy shunt to be sure of having getting rid of any dc component of commercial current probes. The induced voltage in the secondary coil are proportional to the derivative of the flux in the wound core. they are recorded for computing the flux density. Both waves are recorded with an oscilloscope on several periods and 10000 points. The core losses are calculated using (1) and the results are presented in fig.4.

$$P = \frac{1}{T} \int_{(T)} i_p(t) u_s(t) dt \quad (1)$$



Figure 2: MFT prototype made with two high temperature 10 turns coils.

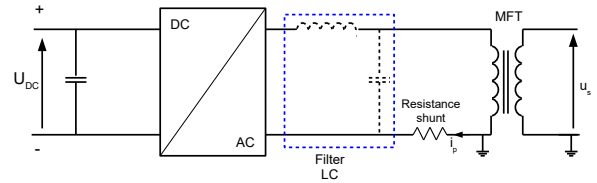


Figure 3: Bloc diagram of the test bench able to perform measurements under rectangular and sine voltages.

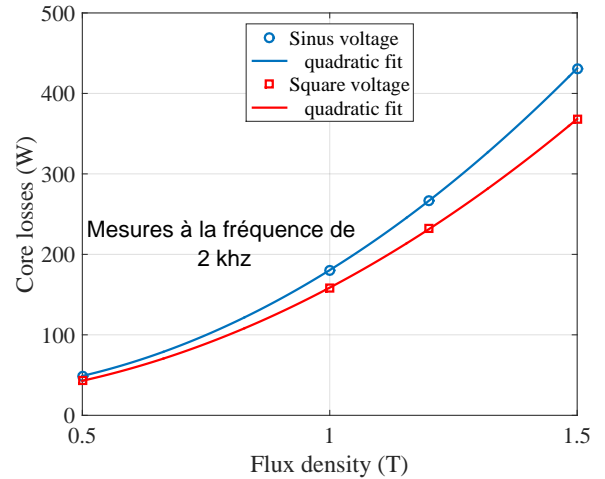


Figure 4: Core losses measured for rectangular and sine voltages at the same peak flux density.

The results show lower core losses for a rectangular voltage, although a square voltage can be described by a number of sinus harmonics, the resulting core losses are compared to a sine one at the same peak flux density. The same tendency is obtained for other frequencies in the kHz range and for larger cores made with the same GOES sheets. These counter-intuitive experimental results need theoretical developments for their interpretation. The general bertotti's

model of core losses in soft magnetic materials shows that the eddy current term becomes preponderant at high [13]. Therefore, the theoretical developments are detailed only for this term.

3. Eddy current losses calculation using Fourier series

The first idea that comes to mind when a sine voltage is compared to a rectangular one is the link with the sum of each the harmonic contribution of its Fourier series. Applying this idea, the total losses for a rectangular voltage should be higher than for a sine one. For GOES wound cores used in the kHz range, the case might be little bit more complex if skin effect occurs. The key point is to perform the comparison at the same peak flux in the core; therefore, the two voltages have different peak values as it can be seen in fig.5.

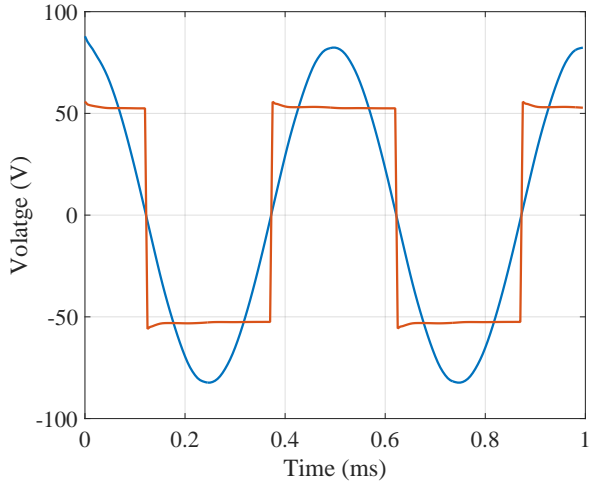


Figure 5: Voltages applied to the primary coil for obtaining the same peak flux density.

In the following, Fourier series are used for calculating the distribution of the magnetic flux density and eddy currents induced by each harmonic inside the GOES lamination. Therefore, it is necessary to assume that the response of any point of the material to an applied magnetic field is linear; this assumption has to be made because the Fourier series are based on the superposition principle, which can only be used for assumed linear properties of the material.

First of all, it should be reminded that the behaviour of the GOES core can be described by the Maxwell equations (2 – 4) where \vec{b} is the magnetic flux density; \vec{h} , the magnetic field strength; \vec{j} , the eddy currents density and \vec{e} , the induced electrical field.

$$\vec{\text{div}}(\vec{b}) = 0 \quad (2)$$

$$\vec{\text{rot}}(\vec{h}) = \vec{j} \quad (3)$$

$$\vec{\text{rot}}(\vec{e}) = -\frac{\partial \vec{b}}{\partial t} \quad (4)$$

The flux density \vec{b} is related to magnetic field \vec{h} by (5), which is a non-linear law in reality (μ depends on \vec{h}); however we assume that the relation is linear for low operating flux density levels:

$$\vec{b} = \mu \vec{h} \quad (5)$$

The eddy currents density are related to the induced electrical field by (6).

$$\vec{j} = \sigma \vec{e} \quad (6)$$

From 2, \vec{b} can be written as the curl of vector potential \vec{a} as following:

$$\vec{b} = \vec{\text{rot}}(\vec{a}) \quad (7)$$

Substituting (7) in (3) and (4), then b using the properties of the curl operator, the equation becomes:

$$\Delta \vec{a} + \mu \sigma \frac{\partial \vec{a}}{\partial t} = \vec{0} \quad (8)$$

The behavior of the wound core is governed by the partial differential equation (8), the problem can be reduced to a 1D differential equation, if we assume that \vec{a} has a single component along the z axis that only changes with the variables (x, t) , with this this assumption (8) becomes :

$$\frac{\partial^2 a_z(x, t)}{\partial x^2} = \mu \sigma \frac{\partial a_z(x, t)}{\partial t} \quad (9)$$

Let $a_0(t)$ be the magnetic vector potential applied on the edges of the GOES wound core, the temporal shape of $a_0(t)$ is triangular because this potential is an image of the flux in the core and, for rectangular voltages, the the flux is triangular.

We also consider that $a_0(t)$ is an odd triangular function; thus it can be written in terms of the Fourier series (10) where \hat{a}_0 is the peak value of the applied magnetic potential, and $k = \{1; 2, 3, \dots\}$.

$$a_0(t) = \sum_{k=0}^{k=N} (-1)^k \frac{8\hat{a}_0}{((2k+1)\pi)^2} \sin((2k+1)\omega t) \quad (10)$$

Each harmonic is a sinusoidal function, therefore, (9) can be written in the complex form (11) where $n = 2k + 1$.

$$\frac{\partial^2 a_{zn}(x)}{\partial x^2} = j\omega_n \mu \sigma a_{zn}(x) \quad (11)$$

Equation (11) is a simple linear differential equation; the variable x stands for the position of any point inside the magnetic sheet, with a reference point $x = 0$ at the centre of the magnetic sheet. The solution can be written as (12) where $\gamma_n^2 = j\omega_n\mu\sigma$. In (12) γ is the complex propagation factor of the damped waves that propagate in the metal thickness from a side of a lamination toward the opposite one. The first term of the sum corresponds to a damped wave propagating in the direction $x > 0$ and the second one in the opposite one.

$$\underline{a}_{zn}(x) = \underline{a}_{1n}e^{-\gamma_n x} + \underline{a}_{2n}e^{\gamma_n x} \quad (12)$$

The complex constants \underline{a}_{1n} and \underline{a}_{2n} can be expressed by (13) where a_{0n} is the peak value of the harmonic component of the magnetic potential imposed on the magnetic sheet surfaces.

$$\underline{a}_{1n} = -\underline{a}_{2n} = -\frac{\underline{a}_{0n}}{2 \sinh(\gamma_n \frac{e}{2})} \quad (13)$$

$$\underline{a}_{0n}(t) = \hat{a}_{0n} e^{j(w_n t + (-1)^{k+1} \frac{\pi}{2})} \quad (14)$$

The magnetic field strength at the edges of the any magnetic sheet is computed from a_{0n} using (5) (7):

$$\underline{h}_{0n}(t) = -\frac{\gamma_n}{\mu \tanh(\gamma_n \frac{e}{2})} \underline{a}_{0n}(t) \quad (15)$$

The magnetic field at each point inside the magnetic sheet, at the instant t can be calculated by (16), which results from the above equations.

$$\underline{h}_{yn}(t)(x) = \underline{h}_{0n}(t) \frac{\cosh(\gamma_n x)}{\cosh(\gamma_n \frac{e}{2})} \quad (16)$$

The flux density is calculated using (5); the eddy currents density is obtained by equation (17) which is deduced from (3).

$$\underline{J}_{zn}(x, t) = -\gamma \underline{h}_{0n}(t) \frac{\sinh(\gamma_n x)}{\cosh(\gamma_n \frac{e}{2})} \quad (17)$$

Returning to the real numbers, distribution of the magnetic field and eddy currents density is obtained by (18) and (19).

$$h(x, t) = \Re \left(\sum_n \underline{h}_n(x, t) e^{j\omega t} \right) \quad (18)$$

$$j(x, t) = \Re \left(\sum_n \underline{J}_n(x, t) e^{j\omega t} \right) \quad (19)$$

The losses are calculated using (20) where N is the number of laminations of the wound core; e , the thickness of a lamination; L_m , mean length of a lamination; L_z , the width of a lamination and ρ , the resistivity of the GOES lamination, its value is $0.48 \times 10^{-6} \Omega m$.

$$p_c(t) = N \times L_m \times L_z \times \int_{-e/2}^{+e/2} \rho j^2(x, t) dx \quad (20)$$

The core losses calculated with Fourier series for 2 kHz and $0.5 T$ is $11.37 W$.

4. Experimental results interpretation with a finite elements (FE) model

4.1. description of the FE model

In order to simulate the behaviour of the GOES wound core, an electromagnetic model based on the FE method has been made. The model considers a portion of one lamination of the core and extrapolate the result to the whole core by assuming that the same phenomena occur in the whole core. Fig.6 presents the principle of the model.

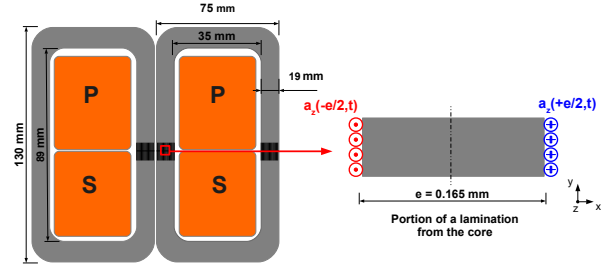


Figure 6: FE model of the wound GOES core.

The core is made of several magnetic sheets insulated between them. It is assumed that the magnetic flux is the same within each lamination, thus we consider a portion of one of them as shown in the fig.6. The model is aimed to calculate the phenomena occurring along the thickness of the lamination (along the x axis), which obey Maxwell equations introduced above.

Taking into account the non-linear relation between the magnetic field and the flux density, eqn. (9) is a non-linear differential equation. This equation is solved in the problem geometry presented in fig.6. The boundary conditions are defined by the potential vector $a_z(\pm \frac{e}{2}, t)$ applied on the edges of the lamination along the z axis. The temporal shape of the potential on the edges is imposed by the flux waveform which depends on the voltage excitation shape. For a rectangular voltage excitation, the flux is triangular thus the applied potential vector on the edges is also triangular, similarly, it is sinusoidal for a sine voltage excitation.

Once (9) is solved, the distribution of \vec{b} along the thickness of the lamination is calculated using (7), and the distribution of the eddy currents density is calculated using (4) by

the following equation :

$$\vec{j} = -\sigma \frac{\partial \vec{a}}{\partial t} \quad (21)$$

The figures 7 and 8 show the distribution the magnetic induction and eddy currents density inside the GOES lamination, at different instants. The square voltage and sinusoidal cases are compared at the same operating frequency and induction peak value, here the values of the operating conditions are respectively 2 kHz and 0.7 T peak flux density. The losses produced inside the core are calculated using (20).

The fig.9 shows the instantaneous core losses calculated for the square voltage and sinusoidal cases at the same operating conditions which are 2 kHz and 0.7 T peak flux density.

The curves in fig. 9 show that for the same operating frequency and peak flux density, the losses induced by the sine voltage are higher than for a he rectangular ones; the average losses are 42 W for sine waves and 32 W for rectangular one.

The fig.10 show losses compared at different peak flux

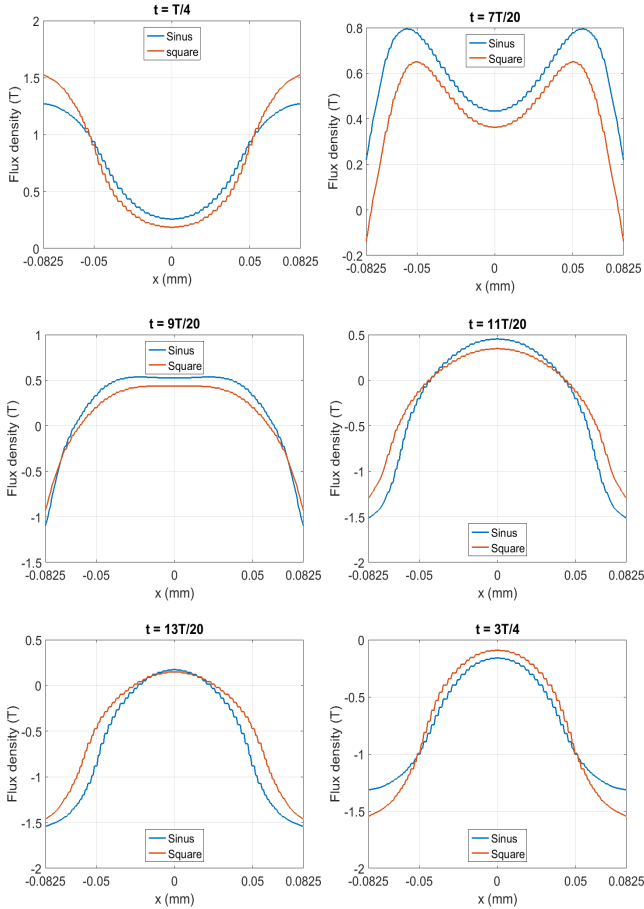


Figure 7: Distribution of the flux density along the thickness of a lamination at different instants, for a rectangular and sine voltage at 2 kHz and 0.7 T peak flux density.

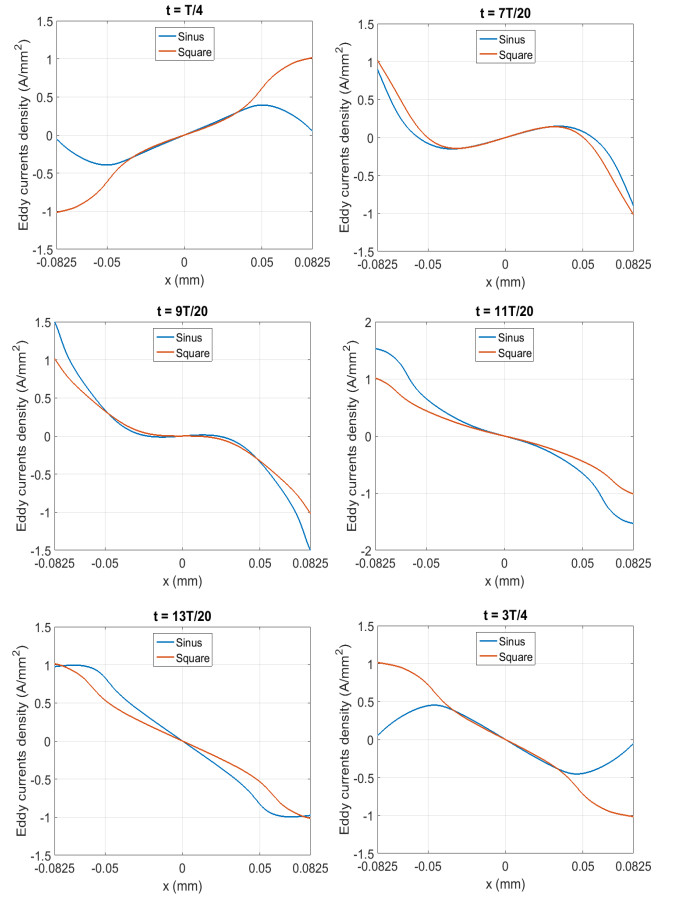


Figure 8: Distribution of eddy currents density along the thickness of a lamination at different instants, for a rectangular and sine voltage at 2 kHz and 0.7 T peak flux density

density for 2 kHz , where it can be seen that the difference increases with the peak flux density for a fixed operating frequency.

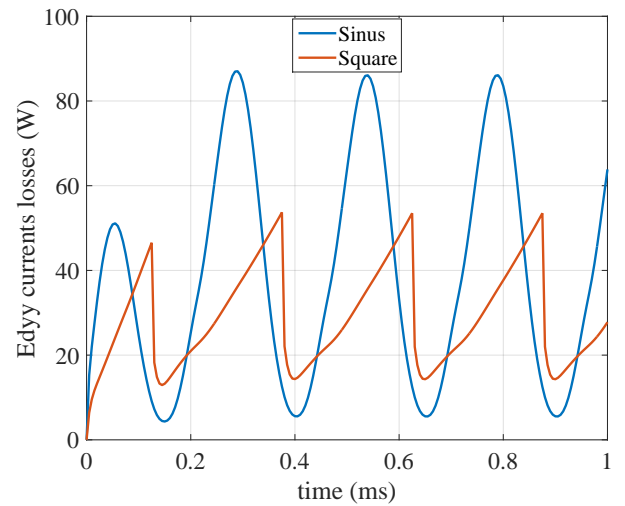


Figure 9: Instantaneous eddy currents losses induced at 2 kHz and 0.7 T peak flux density.

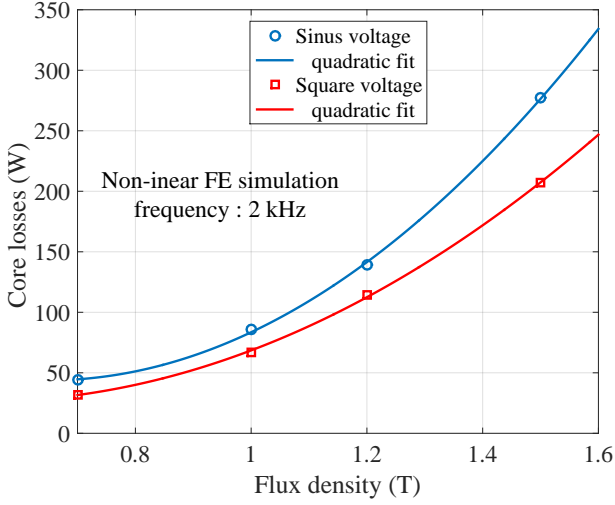


Figure 10: Eddy currents losses for different peak flux density values, at 2 kHz .

The FE model helps to explain the trend between the sinusoidal induced losses and the rectangular ones since it gives the local distribution of the magnetic flux density and the eddy currents, therefore we can see the differences between the two cases at the same operating conditions of the GOES, these differences can be seen in the way which the damped waves propagate inside the GOES thickness, which indicates that the losses aren't necessarily higher in the rectangular case.

The FE elements results give the same trend between the losses induced in the two waves as the experimental results, however, the differences between the values is significant. This could be explained by the fact that the experimental results include the hysteresis and anomalous losses beside the eddy currents contribution, whereas, the FE model assumes that other losses except the eddy currents ones are neglected.

4.2. Comparison of FE and Fourier results

Fig. 11 presents the filed strength on the edges of the GOES wound core and Fig. 12, the average value of the flux density. Results are obtained on the one hand by the FE simulation and on the other hand by Fourier series for 6 harmonics. The operating frequency is 2 kHz and the flux density peak value, 0.5 T .

The value obtained by the linear FE elements simulation is 11.57 W , the difference can be reduced by increasing the number of harmonics. The average losses induced by the sinusoidal excitation calculated using (20) for 2 kHz and 0.5 T is 15 W , it is higher than the rectangular voltage case for the same operating conditions.

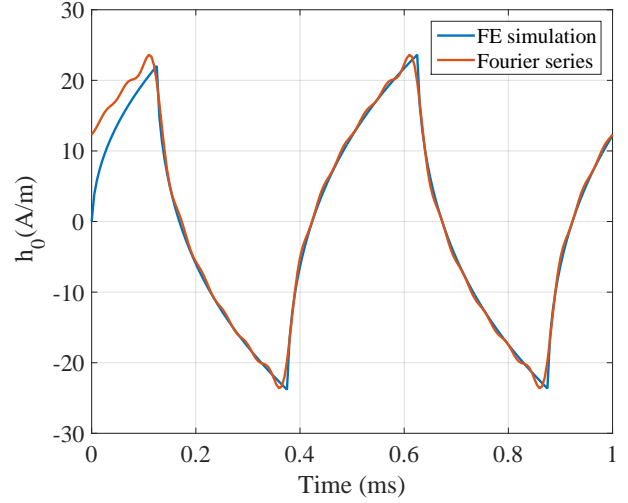


Figure 11: Magnetic field strength at the edges of the wound core, for 2 kHz and 0.5 T .

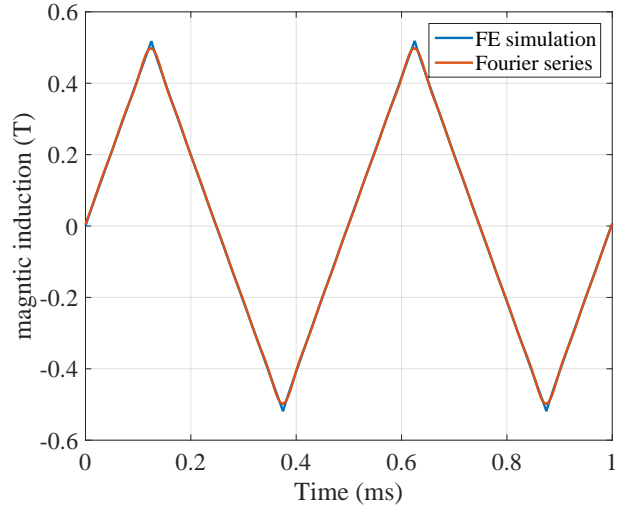


Figure 12: Average flux density in the wound core.

5. Conclusion

The paper shows that, for a GOES wound core at medium frequency and for the same operating frequency and peak flux density, the eddy current losses are lower for rectangular voltages than for sine ones. For linear conditions, Fourier series are used to prove that, even by adding the contribution of each harmonic, the conclusion is the same.

This counter-intuitive result can be explained by the difficult application of Fourier series when a spatial analysis is required at the same time as a frequency one. Indeed, the skin depth is not the same for each harmonic.

The comparison is made for the same peak flux density, which is the practical constraint for the core use, and for the same (f, \hat{b}) the sinusoidal applied voltage peak value is higher than the square one by $\frac{\pi}{2}$, this results in higher level of eddy currents density in the sinusoidal case. This result

is confirmed by the FE simulation, which compares the distribution of eddy currents density inside the GOES and the instantaneous losses curves.

The experimental results show the same trend between the losses induced in the two cases, however, there is an important difference in comparison with the non-linear FE elements modeling results, that could be explained by the fact of non-inclusion contribution of the anomalous and hysteresis losses.

Further works is needed to prove that the anomalous and hysteresis losses contribute in the same way as the eddy currents losses.

Acknowledgment

This work is funded by European funds FEDER and ThyssenKrupp Electrical Steel.

References

- [1] B. D. Cullity and C. D. Graham, *Introduction to magnetic materials*. John Wiley & Sons, 2011.
- [2] J. C. Perrier, A. Lebouc, P. Brissonneau, T. Waeckerle, and J. Verdun, "Magnetic properties of a new grade of thin grain-oriented 3silicon-iron," *IEEE Transactions on Magnetics*, vol. 26, no. 5, pp. 2214–2216, Sep. 1990.
- [3] ABB Business Unit Transformers, *Transformer Handbook*. ABB, 2004. [Online]. Available: <http://www.abb.com/transformers>
- [4] "IEEE standard requirements for tap changers," *IEEE Std C57.131-2012 (Revision of IEEE Std C57.131-1995)*, pp. 1–73, May 2012.
- [5] M. Erol-Kantarci and H. T. Mouftah, "Energy-efficient information and communication infrastructures in the smart grid: A survey on interactions and open issues," *IEEE Communications Surveys Tutorials*, vol. 17, no. 1, pp. 179–197, Firstquarter 2015.
- [6] M. Kuzlu, M. Pipattanasompom, and S. Rahman, "A comprehensive review of smart grid related standards and protocols," in *2017 5th International Istanbul Smart Grid and Cities Congress and Fair (ICSG)*, April 2017, pp. 12–16.
- [7] H. Fan and H. Li, "High-frequency transformer isolated bidirectional dc–dc converter modules with high efficiency over wide load range for 20 kva solid-state transformer," *IEEE Transactions on Power Electronics*, vol. 26, no. 12, pp. 3599–3608, 2011.
- [8] X. She, A. Q. Huang, and R. Burgos, "Review of solid-state transformer technologies and their application in power distribution systems," *IEEE journal of emerging and selected topics in power electronics*, vol. 1, no. 3, pp. 186–198, 2013.
- [9] D. Rothmund, G. Ortiz, T. Guillod, and J. W. Kolar, "10kv sic-based isolated dc-dc converter for medium voltage-connected solid-state transformers," in *2015 IEEE Applied Power Electronics Conference and Exposition (APEC)*. IEEE, 2015, pp. 1096–1103.
- [10] J. W. Kolar and G. Ortiz, "Solid-state-transformers: Key components of future traction and smart grid systems," in *International Power Electronics Conference (IPEC), Hi-roshima*, 2014.
- [11] M. Leibl, G. Ortiz, and J. W. Kolar, "Design and experimental analysis of a medium-frequency transformer for solid-state transformer applications," *IEEE Journal of Emerging and Selected Topics in Power Electronics*, vol. 5, no. 1, pp. 110–123, 2016.
- [12] Z. Xia, Y. Kang, and Q. Wang, "Developments in the production of grain-oriented electrical steel," *Journal of Magnetism and Magnetic Materials*, vol. 320, no. 23, pp. 3229–3233, 2008.
- [13] G. Bertotti, "General properties of power losses in soft ferromagnetic materials," *IEEE Transactions on Magnetics*, vol. 24, no. 1, pp. 621–630, Jan 1988.